Smart Structures and Systems, Vol. 6, No. 4 (2010) 389-403
DOI: http://dx.doi.org/10.12989/sss.2010.6.4.389

Image recognition technology in rotating machinery fault diagnosis based on artificial immune

Zhu Dachang[1]*, Feng Yanping[1], Chen Qiang[1] and Cai Jinbao[2]

[1]*College of Mechanical and Electrical Engineering, Jiangxi University of Science and Technology, Ganzhou, P.R. China*
[2]*Faculty of Foreign Studies, Jiangxi University of Science and Technology, Ganzhou, P.R. China*

(Received November 15, 2007, Accepted September 11, 2009)

Abstract. By using image recognition technology, this paper presents a new fault diagnosis method for rotating machinery with artificial immune algorithm. This method focuses on the vibration state parameter image. The main contribution of this paper is as follows: firstly, 3-D spectrum is created with raw vibrating signals. Secondly, feature information in the state parameter image of rotating machinery is extracted by using Wavelet Packet transformation. Finally, artificial immune algorithm is adopted to diagnose rotating machinery fault. On the modeling of 600MW turbine experimental bench, rotor's normal rate, fault of unbalance, misalignment and bearing pedestal looseness are being examined. It's demonstrated from the diagnosis example of rotating machinery that the proposed method can improve the accuracy rate and diagnosis system robust quality effectively.

Keywords: rotating machinery; fault diagnosis; image recognition technology; artificial immune algorithm.

1. Introduction

Rotating machinery is essential equipment in industries like petrochemical, metallurgy, electric power, aviation, spaceflight, etc. Once the fault happens, it will result in massive economic loss and safety incident. Therefore, the research of fault diagnosis for rotating machinery is important and urgent.

Ordinary diagnosis technique for rotating machinery includes: the diagnosis method based on probability statistics time series model (Upadhyaya and Skorska 1982, Zhinong *et al*. 2006), the pattern recognition method based on Bayesian decision rules (Brandt *et al*. 1997), the signal processing method based on Wavelet Packet analytic fractal geometry (Khan *et al*. 2007), and intelligence diagnosis method based on neural network or artificial immune (Yun *et al.* 2009, Hayashi *et al*. 2002, Tao *et al*. 2006, Elhadet *et al*. 2006). The fault characteristic information which is adopted by diagnosis methods based on knowledge is mainly obtained from the different signal processing technology method, and the heterogeneity fault characteristic often reflects the different aspect of equipment (Kao *et al.* 2009). In former fault diagnosis, it is more convenient to extract information from time waveform, spectrum map and wavelet packet image. Compared with those, some kinds of information especially in the multi-dimension image is hard to be automatically extracted and described in knowledge language. Most of information in multi-dimension images is not utilized sufficiently except that some in 2-D axis orbit feature recognition is finitely utilized. Therefore, diagnosis result is greatly affection; application and

*Corresponding Author, Professor, E-mail: zdc98998@163.com

spreading of diagnosis techniques are limited.

Therefore, according to the experience of image recognition in some fields (Wei *et al*. 2007, Caslellini *et al*. 2000), this paper presents a new fault diagnose method for rotating machinery based on artificial immune - image recognition technique. First, 3-D spectrum parameter image is created after processing raw vibrating signals of rotating machinery, and vibrating data information is collected in the image. 3-D spectrum is transformed into two-dimensions gray scale image according to the characteristic of rotating machinery. Then smoothing, filtering, noise and feature extracting are applied using wavelet packet transformation to directly extract and mine feature information in the state parameter image of rotating machinery. Rotating machinery fault diagnosis is realized by utilization of artificial immune recognition algorithm. A real case of 600MW modulated gas-turbine is studied, including various faults, like unbalance, misalignment, flow-induced vibration and bearing Pedestal looseness. It's demonstrated that this new method is able to improve significantly accurate rate and automatic diagnosis level of fault diagnosis for rotating machinery.

2. Feature extraction based on wavelet packet for rotating machinery fault parameter image

Image recognition technology isn't better utilized in rotating machinery fault diagnosis. One of the primary reasons is that it is difficult to extract image feature. The main fault of the most rotating machinery can be diagnosed through vibration image recognition method. But fault feature in the image can not be inefficiently extracted by use of traditional feature extraction method. The accurate rate of fault diagnosis is very low. Wavelet Packet transformation (Ortiz and Syrmos 2006, Shen *et al*. 2001) is a more meticulous time-frequency analysis means which can efficiently extract all kinds of fault information in rotating machinery vibration image, and which it is an efficient method for fault feature extraction of image. Machinery fault state is shown by every frequency composition energy change in vibration image. From this point, Based on wavelet packet decomposition coefficient single-branch reconstruction, the method that each frequency composition signal's energy is used to build machinery fault feature vector is presented in this paper. The change of energy with each frequency composition is directly used to show machinery fault state in this method which doesn't need systematic model structure.

2.1 Wavelet packet transformation

Wavelet Packet transformation is a time-frequency analysis method of signal. It has merit of multi-resolution analysis and has the capacity of expressing signal local feature in time field and frequency field. Wavelet Packet decomposition can divide frequency band into many layers and further decompose high frequency part which isn't detailed specifically divided in multi-resolution analysis. According to analyzed signal characteristic relative frequency band is elected in self-adapting, which makes Wavelet Packet decomposition match with signal spectrum. Therefore, Wavelet Packet decomposition can detect instantaneous abnormal phenomenon in normal signal and show its composition. When inputting a signal containing abundant frequency composition, owing to Wavelet Packet has different function of restraint and strength for different frequency composition of signal, some frequency composition is restrained and others is strengthened, which makes signal energy to be reduced in some frequency band and to be enhanced in other frequency band. Therefore, energy differentia of each frequency composition can be used to analyze signal differentia (Guohua *et al.* 2006). The image structure and texture are

shown respectively in different frequency band. Contour information is mainly shown in the part of relative lower frequency. Texture details information and all kinds of noises are shown in the part of relative higher frequency. When image texture is clear, the gray scale obviously changes and the contrast gets high in some image fields. It is shown that some feature frequency component is more abundant in frequency field. On the contrary, when image texture is fuzzy, the gray scale unobvious changes and the contrast gets low, opposite feature frequency component is little. Therefore, Wavelet Packet decomposition can be used to obtain relative information which each frequency band contains in image and to analyze image texture feature.

2.2 Feature extraction of image

2.2.1 Extraction of image feature information

Under different work conditions, a group of vibration images are measured as training samples, the samples number is N. Then Image is decomposed by three layers wavelet packet. Image feature of sixteen frequencies from low frequency to high frequency are respectively extracted from the third layer. Its decomposition structure is shown in Fig. 1.

In Fig. 1, the j^{th} node in the i^{th} layer is expressed by (i, j), j=0,1,2,…, 15. Each node stands for specific image feature. (0,0) node stands for original image.

2.2.2 Computing total energy of every frequency band

After decomposing original image by three layers wavelet packet, its wavelet packet coefficients is a two-dimension signal, low frequency coefficients show image texture information, high frequency coefficients show noise. Different articulation of image show different energy in wavelet packet coefficients. If $S_{2,j}$(j=0,1,2,…15) is supposed, corresponding energy is $E_{2,j}$ (j=0,1,2,…,15) which is given by

$$E_{2,j} = \sqrt{\sum_{k=1}^{n}\sum_{l=1}^{m} a_{j,k,l}^2} \tag{1}$$

In the formula, $a_{j,k,l}$(j=0,1,…,15,k=1,2,…,n,l=1,2,…,m) show gray scale of discrete point reconstruction of image. The image size is n×m.

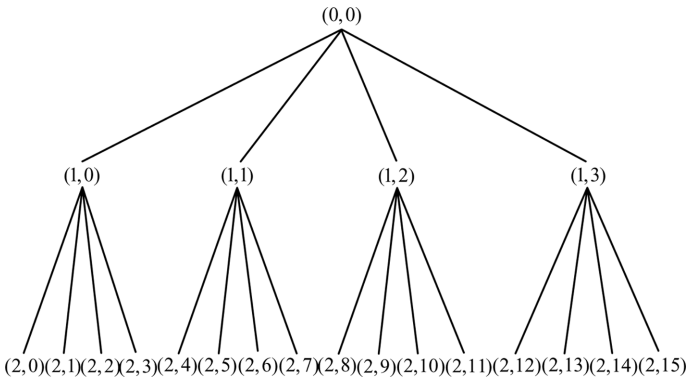

Fig. 1 Three layers Wavelet Packet decomposition of image

2.2.3 Constructing feature vector

Feature vector which shows image feature is constructed by elements which are energy of reconstructed signal which is decomposed by image Wavelet Packet and Feature vector X as follows

X=[$E_{2,0}$, $E_{2,1}$, $E_{2,2}$, $E_{2,3}$, $E_{2,4}$, $E_{2,5}$, $E_{2,6}$, $E_{2,7}$, $E_{2,8}$, $E_{2,9}$, $E_{2,10}$, $E_{2,11}$, $E_{2,12}$, $E_{2,13}$, $E_{2,14}$, $E_{2,15}$]

$$E = \left(\sum_{j=0}^{15} |E_{2,j}|^2 \right)^{1/2} \tag{2}$$

$$X = [E_{2,0}/E, E_{2,1}/E, \ldots E_{2,15}/E] \tag{3}$$

Vector X is the normalization feature vector.

3. Image recognition technology based on artificial immune

The usual methods are Distance function method, Bayesian classification method, fault tree method and so on(,) in fault feature recognition. With the development of theories of fuzzy set, neural network technology and the deepening of relative field subject, such as computer technology and so on. Fault recognition technology is increasingly intellectualized. At present the research results and applications of artificial immune system are relative fewer at home and abroad, because of its complication. Through learning about outside material's natural withstanding mechanism technology, developed artificial immune based on immune mechanism provides evolutionary learning mechanisms of unsupervised learning, self-organizing, etc, and combines with some merits of learning system such as classifier, neural network and so on. It has strong capacity of processing robustness information, and provides a new capacity of solving complex problem. Artificial immune system has successfully been used in some fields such as image recognition, etc. For example, David F. McCoy (McCoy and Devarajan 1997) firstly took negative selection algorithm method to be successfully used in segmentation of remote sensing image in 1997. De Castro (Dasgupta *et al*. 2003) presented clone selection algorithm which has function of continual learning and memory. The algorithm is successfully used in engineering practical problem of character recognition, Multiple Objective Optimization and traveler in 2000. In 2001, Srividhya Sathyanath (Sathyanath and Sahin 2001) took immune genetic algorithm to be successfully used in color image classification, and improved classification accurate rate compared with directly matched algorithm. It took a good foundation for that artificial immune system is successfully used in recognition of rotating machinery state parameter image.

3.1 Artificial immune system mechanism

Biological immune system is a self-adaptive system that has function of learning, memory, pattern recognition and continuous learning from new antigen to improve self immune. Biological immune system is mostly made up of B cells which is produced by the bone marrow. There are 10^{12} different classes B cells in the body. B cell produces Y type antigen in itself surface. Y type antigen is used to recognize and kill some specific antigen. Immune system has maximum merits of immune memory characteristic, antibody self-recognition capability and immune diversity, etc. Antibody recognizing antigen

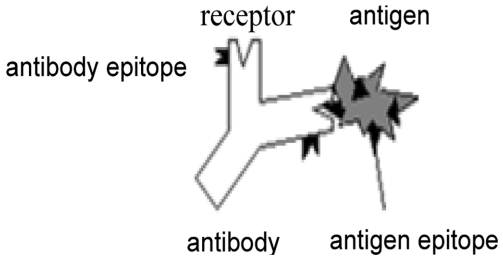

Fig. 2 Antigen and antibody recognition

in immune system is like one key only opening corresponding lock. The matching pattern of antigen and antibody recognition is nearer, the combination intensity is greater, the recognition effect is better, and the affinity of antigen and antibody is greater. Recognition image of antigen and antibody is shown in Fig. 2.

Antigen epitope is the place of being recognized by antibody in antigen surface. Receptor is the place of recognizing antigen epitope in antibody. At the same time, in every kind of antibody this epitope is recognized by other antibody. The epitope is instituted as antibody epitope. Alexander (Tarakanov and Dasgupta 2000) poses energy pattern that antibody recognizes antigen through researching recognition principle between antigen and antibody, he thinks that antigen-antibody couple having the lowest combination energy has the most stable recognition. The pattern as follows

$$w = -u^T M v \tag{4}$$

In this formula, u, $\boldsymbol{v}$ stand for an antigen-antibody recognition couple. $\boldsymbol{u}$, $\boldsymbol{v}$ are unit vector. (namely: $\boldsymbol{uu^T}$=1, $\boldsymbol{vv^T}$=1), the dimension numbers are $\boldsymbol{n_u}$ and $\boldsymbol{n_v}$, M is pattern matrix of combination antigen $\boldsymbol{u}$ with antibody $\boldsymbol{v}$, w stands for combination energy of antigen and antibody.

3.2 Couple of antigen and antibody generation

According to definition of matrix singular value decomposition (Tarakanov and Dasgupta 2000):
If $\boldsymbol{M} \in R^{\mathrm{m\times n}}$, this is an orthogonal matrix, namely

$$U = [u_1, u_2, \ldots, u_m] \subset R^{m \times m}$$

$$V = [v_1, v_2, \ldots, v_n] \subset R^{n \times n} \tag{5}$$

Then

$$M = s_1 u_1 v_1^T + s_2 u_2 v_2^T + \ldots + s_r u_r v_r^T \tag{6}$$

In the formula, $\boldsymbol{s_i}$ is singular value of matrix $\boldsymbol{M}$, $\boldsymbol{u_i}$ and $\boldsymbol{v_i}$ are left singular vector and right singular vector of matrix respectively, $\boldsymbol{r}$ is matrix's rank.

Matrix singular value decomposition has some characters. As follows: $s_1 \geq s_2 \geq \ldots \geq s_r \geq 0$

$$u_i^T u_i = 1, \quad v_i^T v_i = 1, \quad i = 1, 2, \ldots, r$$

$$u_i^T u_j = 0, \quad v_i^T v_j = 0, \quad j \neq i \tag{7}$$

Based on the character of Matrix singular value decomposition, we know: s_1 is further larger than other singular values. If u_i and v_i are regarded as antigen-antibody couple, then w_i is combination energy through matrix M. It is shown in the following formula.

$$w_i = -u_i^T M v_i \tag{8}$$

If using every decomposition item of matrix M for approximating this matrix, then, obtain

$$M \cong s_i u_i v_i^T, \; s_i \cong u_i^T M v_i, \; -s_i \cong -u_i^T M v_i \tag{9}$$

Comparing the formula (8) with the formula (9), it is known that $-s_i$ is combination energy of u_i, v_i. From the formula (7), it is known that only u_1, v_1 have the lowest combination energy (w_{min}) through combining matrix M for all antigen-antibody couples. Obviously, the following formula is right (feasible).

$$w_{\min} = -u_1^T M v_1$$

$$w_{\min} \leq w(u, v), \forall u, v : u^T u = v^T v = 1 \tag{10}$$

Moreover, based on the literature (Zhinong *et al*. 2006), matrix M has the lowest combination energy, when it combines with itself antigen-antibody couple. While it combines with other antigen-antibody couples, matrix M combination energy is higher than the lowest combination energy. When changing combination matrix M, combination energy gets bigger, and change value is higher, then increase amount of combination energy is higher. So that matrix M has the lowest combination energy, only if it combines with itself antigen-antibody couple u_1, v_1.

3.3 Fault diagnosis based on artificial immune

Usually, sample fault feature is given by the form of feature vector. Firstly, fault pattern matrix is constructed based on feature vector of fault sample, for using combination energy in the process of antigen-antibody mutual recognition to realize machinery fault diagnosis.

For every type of fault pattern sample

$$X_{ij} = (x_{ij1}, x_{ij2}, \ldots, x_{ijn})$$

$$i = 1, 2, \ldots, p, j = 1, 2, \ldots, q \tag{11}$$

In the formula, X_{ij} stands for the jth fault sample of the ith type fault, n stands for dimension number of sample feature vector. There is usually many fault samples for every type of fault. Every type of fault pattern sample uses the following method to structure pattern average vector

$$X_i = \left(\sum_{j=1}^{q} x_{ij1} \Big/ j, \sum_{j=1}^{q} x_{ij2} \Big/ j, \ldots, \sum_{j=1}^{q} x_{ijn} \Big/ j \right) \tag{12}$$

Every fault pattern average vector (Dimension number is n.) are demolished and folded into fault

pattern matrixes ($\boldsymbol{M}_1$, $\boldsymbol{M}_2$,…, $\boldsymbol{M}_p$) having $\boldsymbol{n}_1$ row and $\boldsymbol{n}_2$ column. When the dimension number of fault pattern average vector is not decomposed into two integers for multiplication, vector dimension number can be added in the form of complementing zero for pattern average vector in the final, so that it continues to be decomposed.

Then, for every type of fault pattern matrix ($\boldsymbol{M}_1$, $\boldsymbol{M}_2$,…, $\boldsymbol{M}_p$), the number of antigen-antibody couples of every fault pattern is computed through singular value decomposition.

$$(\boldsymbol{u}_{11}, \boldsymbol{v}_{11}), (\boldsymbol{u}_{21}, \boldsymbol{v}_{21}),\ldots,(\boldsymbol{u}_{p1}, \boldsymbol{v}_{p1})$$

Then, above antigen-antibody couples produce memory for all kinds of fault pattern. Learning and training of fault sample are training antigen-antibody couples corresponding to different fault pattern.

In diagnosis, at first, in the same method the sample waiting for diagnosis will be folded into pattern matrix $\boldsymbol{M}^*$ having the same dimension number as fault pattern matrix, then through combining pattern matrix $\boldsymbol{M}^*$ with each kind of training antigen-antibody couple ui1 and vi1 to compute combination energy. Namely

$$w_i = -u_{i1}^T M^* v_{i1} \tag{13}$$

Then, pattern matrix $\boldsymbol{M}^*$ belongs to the type decided by antigen-antibody couple of minimum combination energy. Namely, $M^* \subset class\ (\min(w_i))$.

For practical problem of fault diagnosis, original signal collected by data is time series signal. Normally, original signal is pretreated to produce 3-D spectrum. 3-D spectrum is converted into two-dimension gray scale image according to vibration characteristic of rotating machinery. Wavelet Packet is used for filtering, noise and extracting fault feature then fault sample is generated because original image usually contains a lot of noise composition. After having fault sample containing a lot of fault features, fault diagnosis is carried into execution in term of above introduction method. In the process of diagnosing practical data, fault signal is processed and its feature is extracted in the same method. The process of fault diagnosis is shown in Fig. 3. The left part is off-line learning-training process and the right part is diagnosis process. In practical diagnosis process, the sample needing diagnose only need to combine with the limited antigen-antibody couples (the same as the number of fault type in learning and diagnosing.), which may realize quickly diagnosis.

4. Fault diagnosis instance based on image recognition technology for rotating machinery

In order to prove that this method is effective, four states are tested on rotor-bearing system test-bed of 600 MW supercritical steam unit turbine. Four states are respectively normal state of rotor, rotor unbalanced fault, rotor misalignment fault and bearing loose fault. The component and the link of test-bed installation mainly are shown in Fig. 4. The component contains five parts which are 600 MW supercritical steam unit turbine rotor-bearing system, power system, lubrication system, steam supply system, signal acquisition and analysis system. Fig. 5 is object image of 600 MW supercritical steam unit turbine rotor-bearing system and power system. 600 MW supercritical steam unit turbine rotor-bearing.

The component of test-bed is shown in Fig. 4. It mainly includes five parts: 600 MW super-critical steam unites turbine, power system, lubricating system, airing system and signal gathering and analyzing system. The shafting of Supercritical steam turbine generator unit have nine bearing and five bearing span. The power installation of this test-bed uses 55 KW variable-frequency motor to output rotating

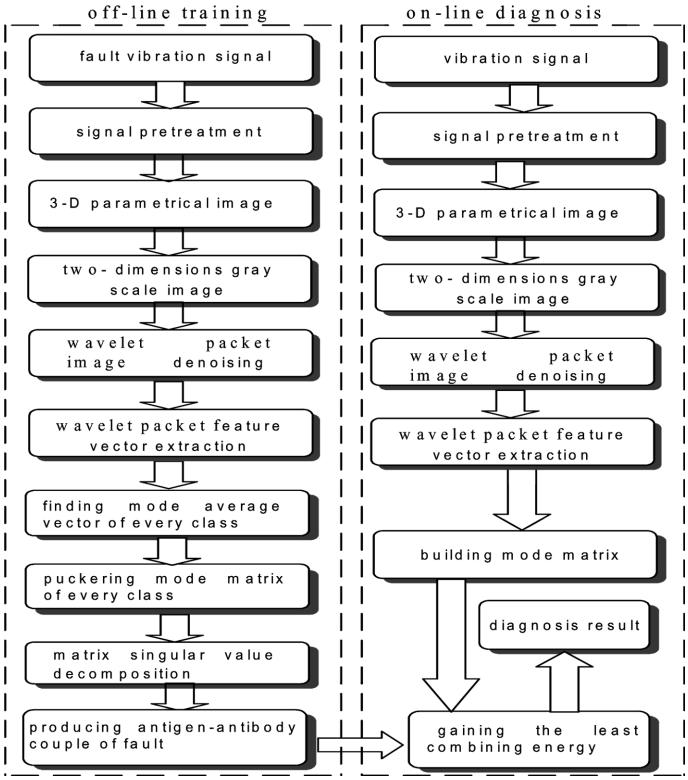

Fig. 3 The block diagram of image recognition based on artificial immune system fault diagnosis

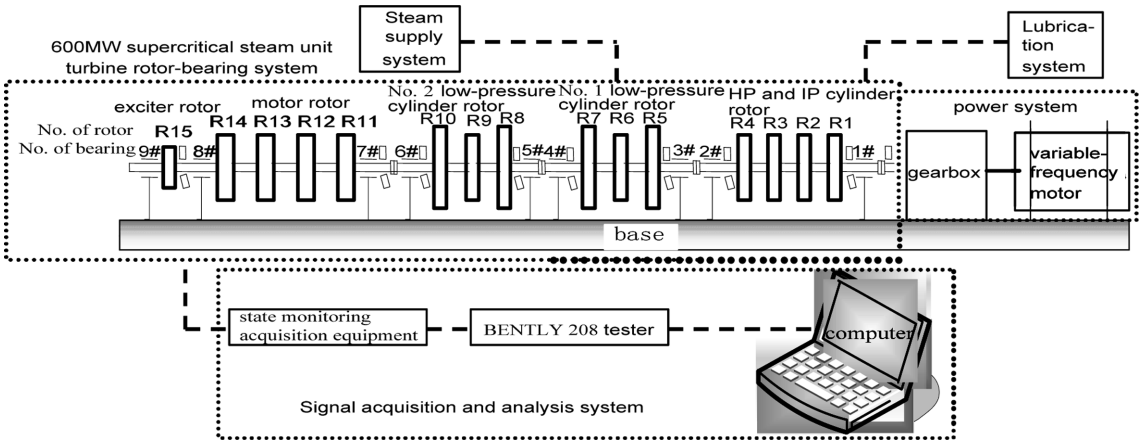

Fig. 4 Test-bed of rotor-bearing system for 600MW supercritical steam turbine unit

speed and power through PRENIC inverter, and uses HG0G-C2 type gearbox. Lubrication system of test-bed supplies oil to every bearing with independence oil supply system. The type of BENTLY3000XL8mm eddy current sensor is installed on every bearing seat which output signal is 7.87 v. In the process of test, the sampling frequency is thirty two times as rotating speed and the sample time is 0.64s. The highest working rotating speed of rotor is 3200 rounds per minute. The

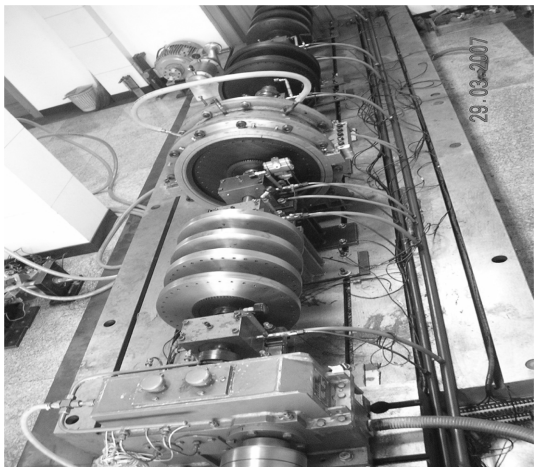

Fig. 5 Rotor-bearing system test-bed of 600MW Supercritical steam unit turbine

collected signals are input into computer by A/D card, which are prepared for data analysis. Otherwise, the type of WP401B oil film pressure sensor and the type of WB2PK-184M3 integration temperature sensor are installed to monitor pressure and temperature of bearing oil.

In order to utilize image recognition method to diagnose fault, four states including normal state of rotor, rotor unbalanced fault, rotor misalignment fault and bearing loose fault are respectively tested. In test, 100 samples of the motor starting and stopping are collected in every state. The total number of samples is 400. In every type of state, 50 samples are learning and training samples, other 50 samples are testing samples. In this paper, every collected original vibration signal sample need retreating, then produces vibration 3-D parameter image (three coordinates are rotating speed and frequency respectively).

Vibration data information is collected in image. From Figs. 6 to 9 are 3-D spectrum of four states (normal state of rotor, rotor unbalanced fault, rotor misalignment fault and bearing loose fault) respectively. 3-D spectrum is converted into two-dimension gray scale image according to rotating machinery image characteristic. Rotating machinery doubling-frequency feature is obvious in 3-D

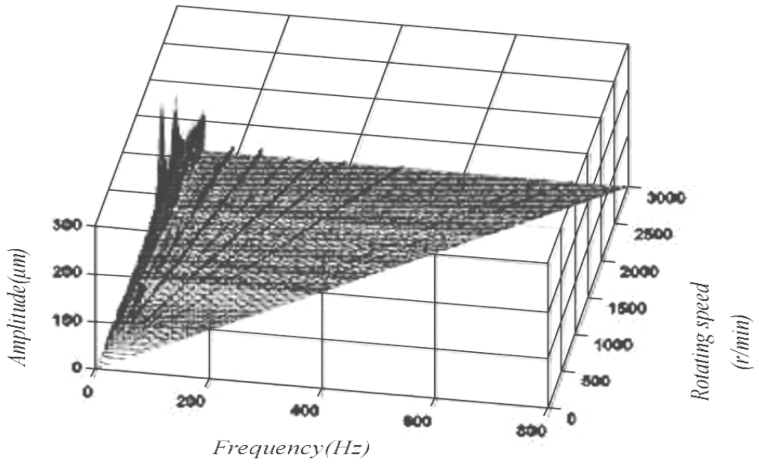

Fig. 6 3-D spectrum of normal rotor vibration

spectrum. Therefore, when being converted, the vertical axle is frequency, horizontal axle is rotating speed. Gray scale of pixel point is amplitude size in this rotating speed and frequency. Obvious vertical line in gray scale image is doubling-frequency line which corresponds with doubling-frequency line in 3-D spectrum. The image is denoised to improve signal-noise ratio because two-dimension image produced by original signal contains noise. This paper adopts noise processing of wavelet packet global threshold. In order to make noise effect better, the image is processed smoothly. Figs. 10 and 11 are processed two-dimension gray scale images of normal rotor and bearing pedestal looseness fault vibration.

Wavelet Packet transformation is used for extracting feature from gray scale image. Feature information of rotating machinery state parameter image is directly extracted and mined. When the energy is higher, it is difficult to analyze data, so feature vectors are normalized. In the process of image feature extraction, the number of layer of wavelet packet decomposition is selected properly. When the number of layer of wavelet packet decomposition is less, image fault feature can not be extracted validly. When the

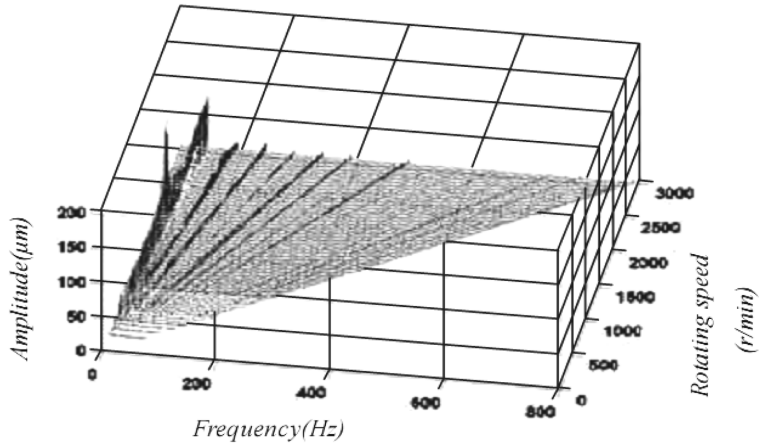

Fig. 7 3-D spectrum of rotor unbalanced fault vibration

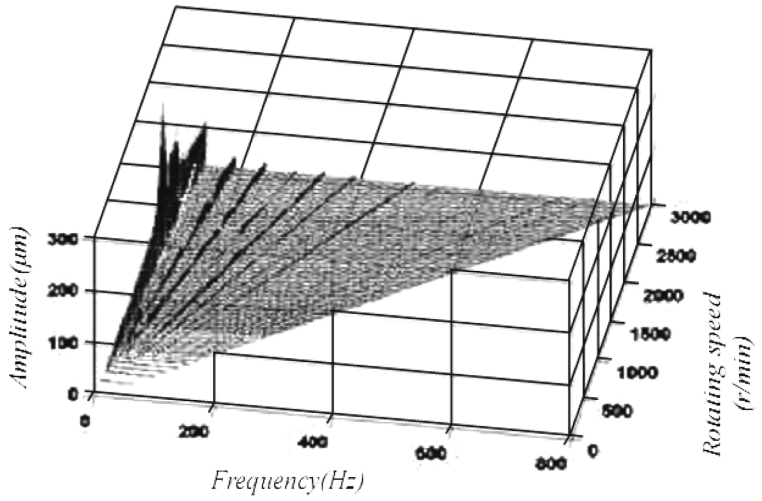

Fig. 8 3-D spectrum of rotor misalignment fault vibration

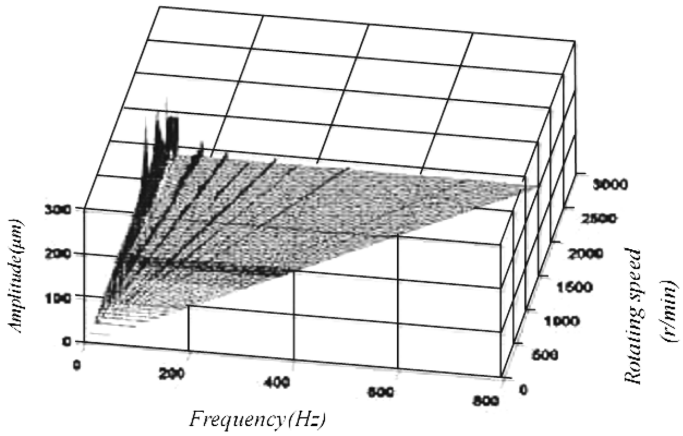

Fig. 9 3-D spectrum of bearing pedestal looseness vibration

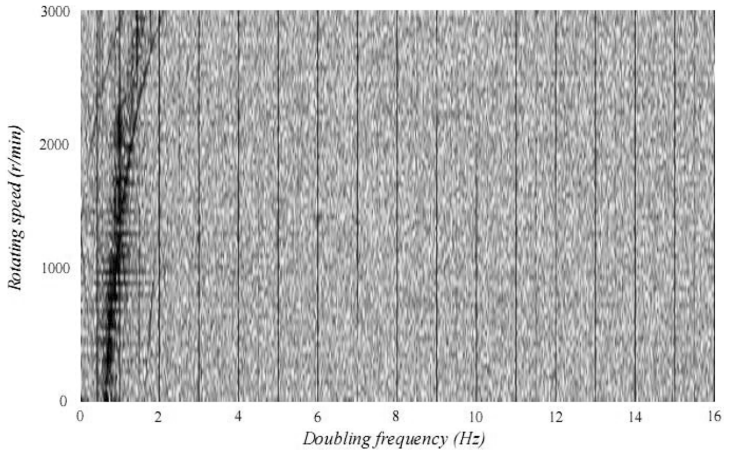

Fig. 10 Gray scale image of normal rotor vibration

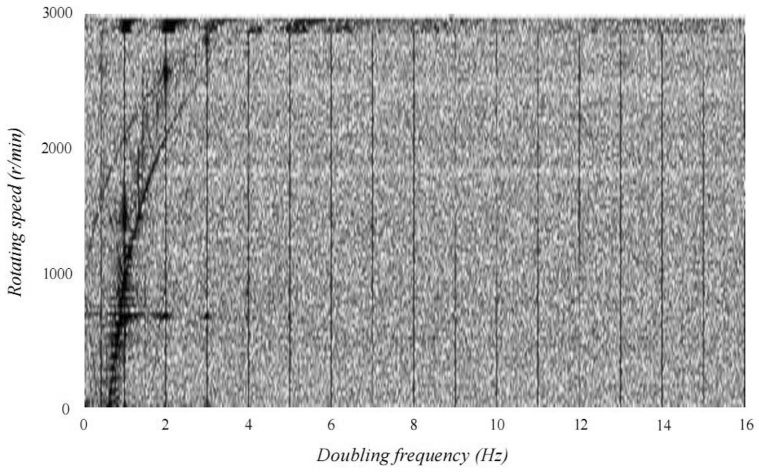

Fig. 11 Gray image of bearing pedestal looseness vibration

number of layer of wavelet packet decomposition is more, the number of dimension of feature vector is bigger, which influences diagnosis speed. According to fault feature of gas-turbine in this paper, 3 layers wavelet packet decomposition are used to extract fault feature, and to produce 16 dimensions feature vector. Many 16 dimensions fault vector sets are obtained through wavelet packet noise and wavelet packet fault feature extraction. Firstly, average vector ($\boldsymbol{X}_1$, $\boldsymbol{X}_2$, $\boldsymbol{X}_3$, $\boldsymbol{X}_4$) of normal pattern and every type of fault pattern are calculated in feature vector sets of 50 training samples. Every type of fault pattern average vector is folded into five fault pattern matrixes of 4×4 ($\boldsymbol{M}_1$, $\boldsymbol{M}_2$, $\boldsymbol{M}_3$, $\boldsymbol{M}_4$).

Then, matrix singular values are decomposed for training Antigen-antibody couples: ($\boldsymbol{u}_1$, $\boldsymbol{v}_1$), ($\boldsymbol{u}_2$, $\boldsymbol{v}_2$), ($\boldsymbol{u}_3$, $\boldsymbol{v}_3$), ($\boldsymbol{u}_4$, $\boldsymbol{v}_4$).

$$\boldsymbol{u}_1 = [-0.9743\ -0.1034\ -0.0144\ -0.0384]$$
$$\boldsymbol{v}_1 = [-0.9863\ -0.0935\ -0.0531\ -0.0171]$$
$$\boldsymbol{u}_2 = [-0.9281\ -0.1743\ -0.0241\ -0.1042]$$
$$\boldsymbol{v}_2 = [-0.8479\ -0.0145\ -0.0151\ -0.0032]$$
$$\boldsymbol{u}_3 = [-0.9874\ -0.2523\ -0.0632\ -0.0042]$$
$$\boldsymbol{v}_3 = [-0.8953\ -0.1063\ -0.0284\ -0.0114]$$
$$\boldsymbol{u}_4 = [-0.9854\ -0.2645\ -0.0436\ -0.0342]$$
$$\boldsymbol{v}_4 = [-0.9963\ -0.1083\ -0.0278\ -0.0197]$$

Every type of 50 testing samples need denoising and feature extraction of wavelet packet too, then every sample is folded into pattern matrix $\boldsymbol{M}^*$. Five trained antigen-antibody couples are combined respectively with pattern matrix $\boldsymbol{M}^*$ so that Antigen-antibody couple having the lowest combination energy is obtained. Fault type which this antigen-antibody couple belongs to is diagnosis result. Diagnosis result is listed in Table 1. Owing to the limitation of paper length, diagnosis result of only 2 testing samples is listed for every type of fault. The accurate rates of diagnosis result are shown in Table 2. The diagnosis result shows: the numbers of mistaken classification of five states testing samples are respectively 2, 1, 4 and 3. The accurate rates are respectively 96%, 98%, 92% and 94%.

Finally, we conduct the online research taking the bearing loose fault as the example, withdraw the

Table 1 Fault diagnosis result of rotor (only given two samples)

State	NO.	Antigen u	Antibody v	W_1	W_2	W_3	W_4	W_5	Result
Normal rotor	1	[-0.9743 -0.1034 -0.0144 -0.0384]	[-0.9863 -0.0935 -0.0531 -0.0171]	**-50.3535**	-50.2156	-10.6543	-50.0135	-50.1006	right
	2			**-50.6431**	-50.1325	-10.8954	-50.4625	-50.5624	right
Rotor unbalanced fault	1	[-0.9281 -0.1743 -0.0241 -0.1042]	[-0.8479 -0.0145 -0.0151 -0.0032]	-52.7842	**-52.9842**	-11.8636	-51.6578	-51.4215	right
	2			-52.5731	-50.9984	**-98.4521**	-51.4878	-52.6424	false
Rotor misalignment fault	1	[-0.9874 -0.2523 -0.0632 -0.0042]	[-0.8953 -0.1063 -0.0284 -0.0114]	-46.7453	-46.8855	**-180.8763**	-47.43645	-47.5224	right
	2			-47.9636	-46.7427	**-360.5321**	-47.8412	-47.3268	right
Bearing Pedestal looseness	1	[-0.9997 -0.1084 -0.0169 -0.0372]	[-0.9883 -0.1084 -0.0182 -0.0276]	-45.5636	-44.9961	-5.7832	-45.2349	-47.9751	right
	2			-45.7231	-45.1548	-5.7451	-45.6254	**-47.7321**	right

Table 2 Statistics of fault diagnosis result

No.	State class	Diagnosis veracity
1	Normal rotor	96%
2	Rotor unbalanced fault	98%
3	Rotor misalignment fault	92%
4	Bearing Pedestal looseness	94%

Table 3 Fault diagnosis result of rotor bearing pedestal looseness

Direction	Mistaken classification sample number	Diagnosis accuracy
0 degree	6	80.0%
45 degree	5	83.3%
90 degree	5	83.3%
135 degree	7	76.7%
Direction fusion	4	86.7%

Table 4 Online fault diagnosis result of rotor bearing pedestal by using artificial immune image recognition method

State class	Mistaken classification sample number	Diagnosis veracity
Normal rotor	3	90.0%
Rotor unbalanced fault	6	80.0%
Rotor misalignment fault	5	83.3%
Bearing Pedestal looseness	4	86.7%

pattern matrix $\boldsymbol{M}^*$ with 4 different direction angles 0, 45, 90, 135 degree. Fault diagnosis result of rotor bearing pedestal looseness is shown in Table 3. In order to eliminate the influence of diagnose result with the direction, fault diagnosis with artificial immune image recognition method applied in online research at the same conditions. Online fault diagnosis result of rotor bearing pedestal by using artificial immune image recognition method is shown in Table 4.

By using artificial immune image recognition method, the mistaken classification sample number cut down to 3, 6, 5 and 4 from the fifty samples and the diagnosis veracity exceed 80 percent. It's demonstrated from the online diagnosis example of rotating machinery that the proposed method can improve the accuracy rate and diagnosis system robust quality effectively.

5. Conclusions

For scarce consideration of multi-dimensions image information, which affects the diagnosis technology promotion and utilization in a certain extent, this paper develops a method which directly extracts and mines texture feature in vibration parameter image for rotating machinery. It presents using the gray co-occurrence matrix for analyzing the texture feature, which describes gray space distribution characteristic and space correlation. At the same time, this method solves the problem that gray co-occurrence matrix is affected by the selected direction. Finally, this paper adopts the artificial immune method to diagnose rotating machinery fault. On the modeling of 600 MW turbine experimental bench,

rotors normal state, fault of unbalance, misalignment and bearing pedestal looseness are being examined. The diagnosis results show that gray co-occurrence matrix combination can obtain more accurate result.

Acknowledgements

This paper is based on the work supported in part by the National Natural Science Foundation of China under Research Grant No. 50965007.

References

Brandt, Y., Jervis, B.W. and Maidon, Y. (1997), "Circuit multi-fault diagnosis and prediction error estimation using a committee of Bayesian neural networks", *Proceedings of the'97 IEE Colloquium on Testing Mixed Signal Circuits and Systems*, London, UK, October.

Caslellini, P., Scalise, A. and Scalise, L. (2000), "A 3-D measurement system for the extraction of diagnostic parameters in suspected skin nevoid lesions", *IEEE T. Instrum. Meas.*, **49**(5), 924-928.

Dasgupta, D., Ji, Z. and Gonzalez, F. (2003), "Artificial immune system (AIS) research in the last five years", *Proceedings of the '03 Congress on Evolutionary Computation*, Canberra, Australia, December.

Elhadet, M., Das, S. and Nayak, A. (2006), "A novel artificial-immune-based approach for system-level fault diagnosis", *Proceedings of the 1st International Conference on Availability, Reliability and Security*, Vienna, Austria, April.

Guohua, Gao, Yu, Zhu, Guanghuang, Duan and Yongzhong, Zhang (2006), "Intelligent fault identification based on wavelet packet energy analysis and SVM", *Proceedings of the '06 9th International Conference on Control, Automation, Robotics and Vision*, Singapore, December.

Hayashi, S., Asakura, T. and Sheng, Zhang (2002), "Study of machine fault diagnosis system using neural networks", *Proceedings of the '02 International Joint Conference on Neural Networks Congress*, Hawaii, USA, May.

Kao, I., Li, X.L. and Tsai, C.H.D. (2009), "Model-based and wavelet-based fault detection and diagnosis for biomedical and manufacturing applications: leading towards better quality of life", *Smart Struct. Syst.*, **5**(2), 153-171.

Khan, M.A.S.K., Radwan, T.S. and Rahman, M.A. (2007), "Real-time implementation of Wavelet packet transform-based diagnosis and protection of three-phase induction motors", *IEEE T. Energy Conver.*, **22**(3), 647-655.

McCoy, D.F. and Devarajan, V. (1997), "Artificial immune systems and aerial image segmentation", *Proceedings of the '97 IEEE International Conference on Systems, Man and Cybernetics*, Hyatt Orlando, Orlando, Florida, USA, October.

Ortiz, E. and Syrmos, V. (2006), "Support vector machines and wavelet packet analysis for fault detection and identification", *Proceedings of the '06 International Joint Conference on Neural Networks Congress*, Vancouver, BC, Canada, July.

Shen, M., Sun, L. and Chan, F.H.Y. (2001), "Method for extracting time-varying rhythms of electroencephalography via wavelet packet analysis", *IEE P.-Sci. Meas. Tech.*, **148**(1), 23-27.

Sathyanath, S. and Sahin, F. (2001), "An AIS approach to a color image classification problem in a real time industrial application", *Proceedings of the '01 IEEE International Conference on Systems, Man and Cybernetics*, Tucson, Arizona, October.

Tao, W., Nian, L., Chi, X. and Kejin, S. (2006), "Study of fault diagnosis in brushless machines based on artificial immune algorithm", *Proceedings of the '06 IEEE International Symposium on Industrial Electronics*, Montreal, Quebec, July.

Tarakanov, A. and Dasgupta, D. (2000), "A formal model of an artificial immune system", *Biosystems*, **55**(1-3),

151-158.
Upadhyaya, B.R. and Skorska, M. (1982), "A modular approach for the diagnostic analysis of dynamic systems using stochastic time-series models", *IEEE T. Syst. Man Cy.*, **12**(6), 794-804.
Wei, Dou, Zhan-sheng, Liu and Xiaowei, Wang (2007), "Application of image recognition based on artificial immune in rotating machinery fault diagnosis", *Proceedings of the 1st International Conference on Bioinformatics and Biomedical Engineering*, Wuhan, China, July.
Yun, G.J., Ogorzalek, K.A., Dyke, S.J. and Song, W. (2009), "A two-stage damage detection approach based on subset selection and genetic algorithms", *Smart Struct. Syst.*, **5**(1), 1-21.
Zhinong, Li, Junjie, Sun and Jie, Han (2006), "Parametric bispectrum analysis of cracked rotor based on blind idendification of time series models", *Proceedings of '06 6th World Congress on Intelligent Control and Automation Congress*, Dalian, China, June.

CC